Draft version October 27, 2010
Preprint typeset using LaTeX style emulateapj v. 4/12/04

Q2122-444: A NAKED AGN FULLY DRESSED

M. Gliozzi
George Mason University, 4400 University Drive, Fairfax, VA 22030

F. Panessa
Istituto di Astrofisica Spaziale e Fisica Cosmica (IASF-INAF), via del Fosso del Cavaliere 100, 00133 Roma, Italy

F. La Franca
Dipartimento di Fisica, Università degli Studi Roma Tre, via della Vasca Navale 84, 00146 Roma, Italy

I. Saviane
ESO - European Southern Observatory, Alonso de Cordova 3107, Casilla 19001, Santiago 19, Chile

L. Monaco
ESO - European Southern Observatory, Alonso de Cordova 3107, Casilla 19001, Santiago 19, Chile

L. Foschini
INAF - Osservatorio Astronomico di Brera, via E. Bianchi 46, I-23807 Merate, Italy

L. Kedziora-Chudczer
Australia Telescope National Facility, CSIRO, P.O. Box 76, Epping, NSW 1710 *Currently at the School of Physics, UNSW, Sydney, NSW 2052 Australia*

S. Satyapal
George Mason University, 4400 University Drive, Fairfax, VA 22030

R.M. Sambruna
NASA's Goddard Space Flight Center, Code 661, Greenbelt, MD 20771
Draft version October 27, 2010

ABSTRACT

Based on previous spectral and temporal optical studies, Q2122-444 has been classified as a naked AGN or true type 2 AGN, that is, an AGN that genuinely lacks a broad line region (BLR). Its optical spectrum seemed to possess only narrow forbidden emission lines that are typical of type 2 (obscured) AGNs, but the long-term optical light curve, obtained from a monitoring campaign over more than two decades, showed strong variability, apparently ruling out the presence of heavy obscuration. Here, we present the results from a ∼40 ks XMM-Newton observation of Q2122-444 carried out to shed light on the energetics of this enigmatic AGN. The X-ray analysis was complemented with ATCA radio data to assess the possible presence of a jet, and with new NTT/EFOSC2 optical spectroscopic data to verify the actual absence of a BLR. The higher-quality optical data revealed the presence of strong and broad Balmer lines that are at odds with the previous spectral classification of this AGN. The lack of detection of radio emission rules out the presence of a jet. The X-ray data combined with simultaneous UV observations carried out by the OM aboard *XMM-Newton* confirm that Q2122-444 is a typical type-1 AGN without any significant intrinsic absorption. New estimates of the black hole mass independently obtained from the broad Balmer lines and from a new scaling technique based on X-ray spectral data suggest that Q2122–444 is accreting at a relatively high rate in Eddington units.
Subject headings: Galaxies: active – Galaxies: nuclei – X-rays: galaxies

1. INTRODUCTION

More than two decades of multi-wavelength observations and theoretical studies have led to a generally accepted unification scheme for AGNs. According to this scheme, all AGNs share some basic ingredients: 1) a supermassive black hole; 2) an accretion disk coupled with a hot corona, which radiates from the optical through X-ray energies; 3) high velocity and high density gas located at ∼ pc scales, usually referred to as broad-line region (BLR), since its radiation is dominated by broad (FWHM∼ 2000–10,000 km s^{-1}) permitted lines; 4) lower velocity and low density gas located at ∼ kpc scales, referred to as narrow-line region (NLR), and emitting narrow (FWHM< 1000 km s^{-1}) forbidden

and permitted lines. A gaseous and molecular torus on pc scales presumably obscures the inner engine and the BLR when viewed edge-on. In addition, in $\sim$ 10% of AGNs, there are relativistic jets extending from kpc up to Mpc scales. Within this scheme, several observational differences in the broad-band and line spectral properties between type 1 (objects with broad permitted lines) and type 2 AGNs (with narrow lines only; see Osterbrock 1981) are explained by orientation effects (e.g. Antonucci 1993; Urry & Padovani 1995).

Although observations generally support orientation-based unification models for AGNs, exceptions do exist (e.g. Pappa et al. 2001; Panessa & Bassani 2002; Bianchi et al. 2008; Trump et al. 2009). Observationally, only about 50% of the brightest Seyfert 2s show the presence of hidden broad line regions (HBLRs; Tran 2001) in their polarized optical spectra. Several studies suggest that the presence or absence of HBLRs depends on the AGN luminosity, with HBLR sources having larger optical luminosities (e.g. Tran 2001; Gu & Huang 2002). From the theoretical view point, Nicastro (2000) hypothesized that the absence of HBLRs corresponds to low values for accretion rate onto the central black hole. Similar conclusions are reached by Elitzur & Ho (2009) in the context of the disk-wind scenario for low accretion rate AGNs. Further support for the existence of AGNs lacking a BLR was put forward by Hawkins (2004), who reported the discovery of six naked AGNs – a new class of AGNs characterized by the absence of the broad line region accompanied by strong continuum emission and strong variability in the optical band. This result is based on a large-scale monitoring program carried out in different optical bands over the last 25 years, and on the spectroscopic follow-up (see Hawkins 2004 and references therein for a more detailed description of the optical observations).

It must be outlined that, although the unification models are able to explain most of the AGN observational properties, they do not offer any insight into the physical origin of the basic AGN ingredients, namely the BLR, the NLR, accretion flow, and the torus. Detailed investigations of AGNs without BLR have the potential of shedding some light on the physical mechanisms that lead to the suppression (and possibly also to the formation) of the BLR. In addition, in the framework of clumpy torus models (e.g. Nenkova et al. 2002), there is growing evidence that the torus and the BLR are not separate entities. Therefore, the study of naked AGNs may provide useful constraints also on the formation mechanism and nature of the torus. Finally, if indeed naked AGNs lack BLR and strong intrinsic absorption, they offer the best opportunity to investigate the accretion flow. An additional (and perhaps the most important) reason is that AGNs without BLR might be representative of a large class of AGNs and thus a detailed study of the naked AGNs is critical. Indeed, recent studies of Steffen et al. (2003), based on Chandra deep field data, indicate that a sizable fraction of the local AGN population is without BLs and in fact represents the dominant AGN class for X-ray luminosities below $\sim 4 \times 10^{43}$ erg s^{-1} (see also Lawrence & Elvis 1982; La Franca et al. 2005). This is consistent with the findings of several recent studies (e.g. Bian & Gu 2007; Diamond-Stanic et al. 2009; Plotkin et al. 2010) that suggest that AGNs without BLR or with weak optical lines are associated not only with low-luminosity AGNs but also with relatively bright AGNs.

One of the most effective ways to investigate the properties of AGNs is with X-ray observations, since X-rays are produced and reprocessed in the inner, hottest nuclear regions of the source, and their penetrating power allows them to carry information from the central engine without being substantially affected by absorption, and to probe the presence of the putative torus.

Recently, we carried out a preliminary X-ray study of three naked AGNs (Q2122-444, Q2130-431, Q2131-427) with *Chandra* snapshot observations that were performed in December 2005. The most relevant results from the *Chandra* study are reported in Gliozzi et al. (2007) and can be summarized as follows: (1) The three AGNs are easily detected in X-rays and appear to be point-like at the sub-arcsecond resolution of *Chandra*. (2) Their X-ray spectral properties are consistent with those of Seyfert 1 galaxies, with typical photon indices of $\sim$1.8 and without strong intrinsic absorption ($N_{\rm H} < 5 \times 10^{21}$ cm^{-2}). (3) The three sources are fairly bright in the X-rays with values comparable with those observed in Seyfert 1 galaxies and larger than typical Seyfert 2 luminosities (Turner et al. 1997), and have Eddington ratios ranging between 10^{-4} and 10^{-2} .

More recently, Q2131-427 and Q2130-431, two of the original naked AGNs detected by Hawkins (2004), have been observed quasi-simultaneously in the X-rays with *XMM-Newton* and in the optical band with the NTT by Panessa et al. (2009). The high-quality optical spectroscopic data confirmed the "naked" nature of Q2131-427 but revealed weak broad lines for Q2130-431. On one hand, these results combined with the lack of intrinsic absorption inferred from *XMM-Newton* led Panessa et al. (2009) to the conclusion that Q2131-427 is a "true" type 2 AGN and Q2130-431 might be a "true" intermediate Seyfert with an intrinsically weak BLR. On the other hand, the detection of broad lines in the optical spectrum of Q2130-431 casts some doubts on the optical classification of the original sample of Hawkins (2004), since it is based on relatively low-sensitivity optical spectral data.

Here we investigate the nature of the central engine in Q2122–444 ($\rm RA_{J2000} = 21^h26^m03.94^s$, $\rm Dec_{J2000} = -44^o11'19"$, z=0.311), another putative naked AGN from the sample of Hawkins (2004). To this end we make use of *XMM-Newton* EPIC and OM data (described in Section 3) to shed light on the energetics of this enigmatic AGN. The *XMM-Newton* analysis is complemented with the investigation of new optical spectroscopic data recently obtained from the NTT/EFOSC2 to robustly verify the claim that Q2122–444 lacks a BLR (see Sect. 4). We also use radio data from the Australia Telescope Compact Array (ATCA) to assess whether the peculiar properties of this source can be explained by the presence of a jet. The description of all the observations and the data reduction is provided in Section 2. The main results and their implications are discussed in Section 5, while the main conclusions are summarized in Section 6.

2. OBSERVATIONS AND DATA REDUCTION

2.1. *XMM-Newton*

Q2122–444 was observed by *XMM-Newton* from November 18, 2007, 22:38 UT to November 19, 2007, 10:22 UT. The EPIC pn and MOS cameras were operated in full-frame mode with a thin filter. The data were processed using the latest CCD gain values. For the temporal and spectral analysis, events corresponding to pattern 0–12 (singles, doubles, triples, and quadruples) in the MOS cameras and 0–4 (singles and doubles only, since the pn pixels are larger) in the pn camera were accepted. Arf and rmf files were created with the *XMM-Newton* Science Analysis Software (`SAS`) 8.0. The recorded events were screened to remove known hot pixels and data affected by periods of flaring background. The resulting effective total exposures are 34 ks for the EPIC pn and 41 ks for both MOS cameras. The extraction radius used for the source spectra and light curves is 30″. Background spectra and light curves were extracted from source-free circular regions of 60″ extraction radius on the same chip as the source. There are no signs of pile-up in the pn or MOS cameras according to the `SAS` task `epatplot`. The RGS data have signal-to-noise ratio (S/N) that is too low for a meaningful analysis.

The X-ray spectral analysis was performed using the `XSPEC v.12.4.0` software package (Arnaud 1996). The EPIC data have been re-binned in order to contain at least 20 counts per channel for the χ^2 statistic to be valid. The errors on spectral parameters are at 90% confidence level for one interesting parameter ($\Delta\chi^2 = 2.71$).

The data from the OM (Mason et al. 2001) were processed with the latest calibration files using the `SAS` task `omichain`, which provides count rates in the B, U, UVW1, and UVM2 bands. The count rates were then converted into magnitudes using the formula mag $= -2.5\log$(count rate) + zeropoint (where the zeropoints are 19.266, 18.259, 17.204, and 15.772, for the B, U, UVW1, and UVM2 bands, respectively) and corrected for systematics. The values were corrected for extinction (see Sect 3.3 for more details) and converted to fluxes by using standard formulae (e.g. Zombeck 1990).

2.2. *NTT/EFOSC2*

The optical spectroscopic data of Q2122–444 were retrieved from the ESO archive. Q2122–444 was observed with ESO Faint Object Spectrograph and Camera v.2 (EFOSC2) at the New Technology Telescope (NTT) in La Silla (Chile) on 2009, July 6th with grating #13 and a 1-arcsec slit width which corresponds to a wavelength resolution of 21.2 Å (FWHM), in the range 3900-9200 Å. Three spectra with exposure time of 600s each were acquired (air mass $\sim$ 1.08). A standard reduction process was applied using midas and iraf tasks. The raw data were bias subtracted, cleaned from cosmic rays and corrected for pixel-to-pixel variations (flat-field). Object spectra were extracted and sky subtracted. Eventually the three spectra were averaged to obtain a single higher S/N spectrum. Wavelength calibrations were carried out by comparison with exposures of He and Ar lamps, with an accuracy $<$ 15 Å. Relative flux calibration was carried out by observations of several spectrophotometric standard stars (Oke 1990).

2.3. *ATCA*

We used the ATCA in the 6A configuration for imaging Q2122–444 at 4.8 and 8.6 GHz. The beam size at 8.6 GHz is 1.3×0.8″ with a position angle of 78.9^o. At 4.8 GHz the beam size is 2.2×1.4″ with a position angle of 58.9^o. Typically the positional accuracy may be affected by pointing stability of the array. However, the pointing deviations are usually below 1 arcsec even for the snapshot observations. The source was observed in three sessions over the period between 20 and 22 Jan 2008. In each session we obtained six 10-minutes scans with 1 second integration time at each frequency, which were interleaved with the observations of the point source phase calibrator, PKS 2106-413. The flux density calibration was achieved with the ATCA primary calibrator, PKS 1934-638. The final images of the 30 (15) arcsec area for 4.8 (8.6) GHz around the optical position of the source show no detection of radio emission above the 0.78 mJy noise level limit (which is the 3 sigma flux limit).

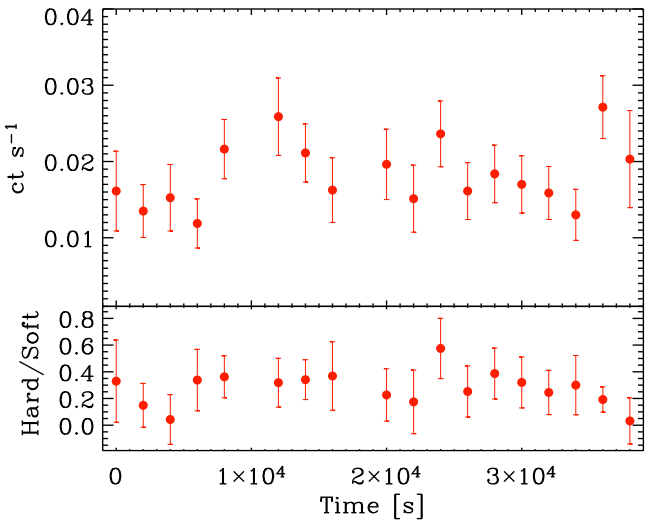

FIG. 1.— *XMM-Newton* EPIC light curve in the 0.3–10 keV (top panel), and HR=(2–10 keV/0.3–2 keV) plotted versus the time (bottom panel) for Q2122–444.

3. THE XMM-NEWTON VIEW OF Q2122–444

3.1. *X-ray temporal analysis of Q2122–444*

We studied the short-term variability of Q2122–444 using EPIC pn data with time-bins of 2000 s. Figure 1 shows the EPIC time series of the 0.3-10 keV band (top panel) and of the hardness ratio HR =2-10 keV/0.3-2 keV (bottom panel). A visual inspection of Fig. 1 suggests that low-amplitude flux changes might be present in the light curve without being accompanied by spectral variations. A formal analysis based on a χ^2 test indicates that there is no significant temporal ($P_{\chi^2} \simeq 32\%$) or spectral ($P_{\chi^2} \simeq 92\%$) variability on short timescales.

Since Q2122–444 has also been observed by *Chandra* in December 2005, it is possible to investigate the presence of long-term flux variations. Over a period of nearly two years the 2–10 keV flux of Q2122–444 decreased by a factor of $\sim$2 (from 7.4×10^{-14} erg cm^{-2} s^{-1} measured during the *Chandra* snapshot survey to 3.9×10^{-14} erg cm^{-2} s^{-1} measured by *XMM-Newton*). Interestingly, this significant change of X-ray flux appears to be accompanied by a moderate spectral vari-

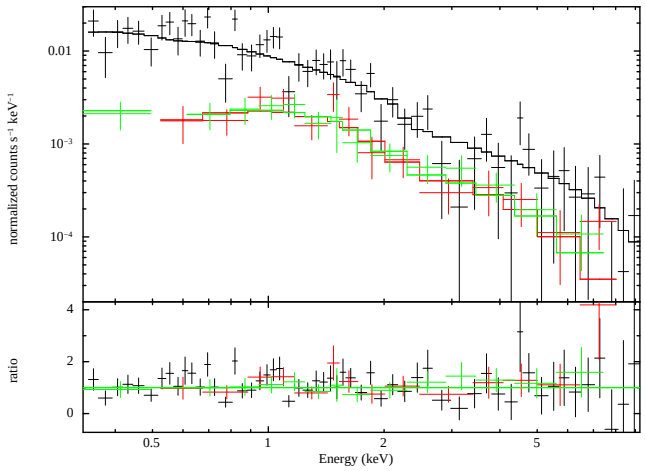

FIG. 2.— EPIC spectra of Q2122-444 and data/model ratios to a simple power-law model modified by photoelectric absorption. Black, red, and green symbols represent the EPIC pn, MOS1, and MOS2 data, respectively.

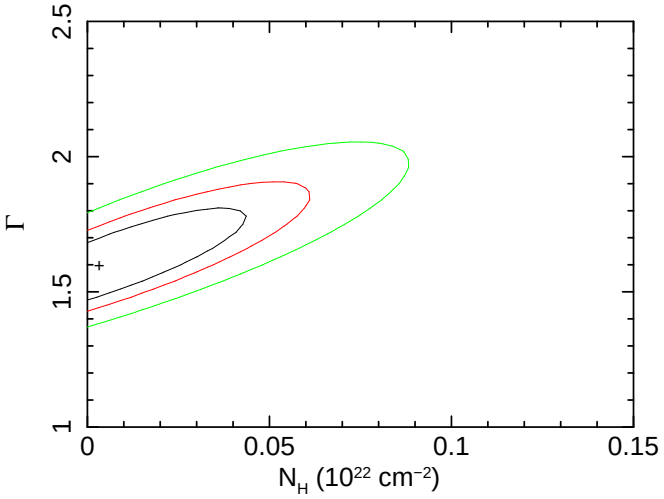

FIG. 3.— Confidence contours (68%, 90%, and 99%) in the Γ – $N_{\rm H}$ plane for Q2122-444.

ability: the hardness ratio of Q2122–444 increases from $HR_{\rm Chandra} = 0.27 \pm 0.11$ to $HR_{\rm XMM} = 0.60 \pm 0.04$. This suggests that Q2122–444 follows the typical spectral variability trend observed in Seyfert 1 galaxies, with a steeper X-ray spectrum when the source is brighter (e.g. Sobolewska & Papadakis 2009).

3.2. *X-ray spectral analysis of Q2122–444*

Unlike the *Chandra* spectral analysis that was severely hampered by poor photon statistics due to the brevity of the observation, the longer *XMM-Newton* exposure coupled with its high throughput makes it possible to study the X-ray spectral properties of Q2122–444 in greater detail. However, similar to the *Chandra* ACIS spectrum, the combined spectra of the three EPIC cameras are adequately fitted by a simple power law modified by absorption that is left free to vary ($\chi^2_{\rm red} = 1.05$; 112 d.o.f). The best-fit values of the relevant spectral parameters are: $\Gamma = 1.62 \pm 0.14$ and $N_{\rm H} = 8^{+23}_{-8} \times 10^{19}$ cm^{-2}. Similar values of Γ and $\chi^2_{\rm red}$ are obtained when the column density is fixed at the Galactic value 3.6×10^{20} cm^{-2}. The spectra and residuals of Q2122-444 are shown in Figure 2, while Figure 3 shows the confidence contours of Γ and $N_{\rm H}$.

It is instructive to compare these results with the corresponding ones obtained with the *Chandra* snapshots (see Figs. 2 and 3 from Gliozzi et al. 2007). Although the parameters from the *XMM-Newton* analysis are more tightly constrained, the basic conclusions remain the same: the photon index is consistent with typical values measured in Seyfert 1 galaxies and, more importantly, there is no evidence for intrinsic absorption (the 90% confidence contours are fully consistent with the Galactic value, $N_{\rm H,Gal} = 3.6 \times 10^{20}$ cm^{-2}).

Although the EPIC cameras have a larger effective area above 6 keV with respect to the *Chandra* ACIS camera, the limited statistics of the *XMM-Newton* spectrum of Q2122–444 does not allow a detailed investigation of the Fe Kα line. The line energy and width remain unconstrained when they are left free to vary, therefore we fixed them at $E = 6.4$ keV and σ=0.01 keV, respectively. The model comprising a Fe Kα line in addition to the absorbed power law does not lead to any statistically significant improvement of the fit ($\Delta\chi^2 \simeq 1$ for one additional parameter) indicating that a Fe Kα line is not required. The equivalent width of this line is 640 eV with a 90% upper limit of $\sim$1 keV.

Since the X-ray emission is likely to be produced by the Comptonization of seed photons emitted by the underlying accretion disk, it is appropriate and physically more motivated to use a Comptonization model instead of a phenomenological model like the power law. Using a general Comptonization model, the Bulk Motion Comptonization (BMC; Titarchuk et al. 1997), yields a fit ($\chi^2_{\rm red} = 1.08$; 110 d.o.f) which is statistically indistinguishable from the power law fit, with parameters that are fairly typical for AGNs. Specifically, we obtain $kT = 0.1$ keV (the temperature of the seed photons), $\alpha = 0.63 \pm 0.14$ (the spectral index, which is related to the photon index by $\Gamma = \alpha + 1$), $\log A = 0.11$ (which is related to the Comptonization fraction f by the relation $f = A/(1 + A)$, where f is the ratio of Compton scattered photons over the seed photons), and the normalization $N_{\rm BMC} = (2.8 \pm 0.2) \times 10^{-7}$, which is in units of $(L/10^{39}$ erg s$^{-1})(10$ kpc$/d)^2$ with L and d being the luminosity and distance of the object, respectively.

The use of the BMC model is the first step necessary to constrain the black hole mass in Q2122–444. The estimate $M_{\rm BH}$ is obtained from the X-ray spectral results of the BMC model by making use of a scaling technique recently introduced for Galactic black holes by Shaposhnikov & Titarchuk (2009) and extended to AGNs by Gliozzi et al. (2010). This procedure is described in Section 5.

3.3. *The OM view of Q2122–444*

The simultaneous use of several cameras and telescopes on board of *XMM-Newton* is one of the most beneficial capability of this satellite. This property not only makes it possible to increase the S/N in the X-ray band by combining the data of the three EPIC cameras, but thanks

to the OM it also offers the simultaneous coverage of the optical and UV bands, which is crucial to understand the energetics of AGNs.

During the *XMM-Newton* pointing in November 2007, the OM detected Q2122–444 in the B (4400 Å), U (3440 Å), and UVW1 (2910 Å) bands, whereas the source was not detected with the UVW2 (2120 Å) filter. The observed magnitudes are respectively: $m_B = 21.1 \pm 0.4$, $m_U = 20.2 \pm 0.2$, $m_{UVW1} = 20.1 \pm 0.2$. Since there is no general consensus on the extinction corrections that need to be applied in the optical-UV band, we have tried different extinction curves, including the Galactic extinction proposed by Cardelli et al. (1989) and the Small Magellanic Cloud (SMC) type extinction (Prevot et al. 1984), which proved to work well on a large sample of AGNs from the Sloan Digital Sky Survey (Hopkins et al. 2004). For completeness, we also applied extinction corrections derived from the X-ray spectral fits by converting $N_{\rm H}$ into optical extinction with the relation $A(V)/N_{\rm H} = 5.3 \times 10^{-22}$ (Cox & Allen 2000). The results from the different extinction laws are consistent with each other within 10%.

One of the most widely used quantities to parametrize the broadband properties of AGNs is the the spectral index, $\alpha_{\rm OX} = -\log(l_{2500\mathring{\rm A}}/l_{2\rm keV})/\log(\nu_{2500\mathring{\rm A}}/\nu_{2\rm keV})$ (Tananbaum et al. 1979). We derive $\alpha_{\rm OX} = 1.31 \pm 0.06$, from the simultaneous X-ray and UV (UVW1 filter) fluxes, assuming a typical UV slope of 0.7 ($f_\nu \propto \nu^{-0.7}$) and the extinction prescriptions discussed above. In Section 5 we discuss the implications of this result in the context of type 1 AGNs.

4. OPTICAL SPECTROSCOPY OF Q2122–444

In Figure 4 we show the EFOSC2 optical spectrum of Q2122–444. The line intensities and widths were measured by fitting Gaussian profiles and the Full Width Half Maximum (FWHM) calculated taking into account the spectrograph resolution. The results from the spectral fitting of the relevant lines are shown in Table 1.

The presence of strong broad Balmer lines clearly points to a reclassification of Q2122–444 as a type 1 Seyfert galaxy. Hawkins (2004) measured a FWHM of 351 km/s and 699 km/s for the H_β and [O III] emission lines respectively (the H_α line was out of the covered spectral range) and classified this source as a type 2 AGN. A possible explanation for the mis-match between the two optical classifications is that the H_β broad component may have been obscured by a nearby absorber at the time of the Hawkins observation, in agreement with the findings of Risaliti et al. (2009) that demonstrate that variations of the local absorber can occur on short timescales and change the appearance of the central engine. In addition, it must be pointed out that Hawkins' optical spectroscopy was performed with a 2dF multi-fibre spectrograph at the AAT which cannot guarantee high S/N ratio spectra because of difficulties in subtracting the sky background (e.g. Lissandrini et al. 1994; Watson et al. 1998), and this problem is more severe for relatively faint objects like Q2122–444.

5. DISCUSSION

The primary goal of our original *XMM-Newton* project was to shed light on the nature of Q2122–444, a member

TABLE 1
Measured line parameters for the optical spectrum of Q2122–444.

Line	Flux (10^{-15} cgs)	FWHM (km s^{-1})	EW (Å)
H_α	7.87±0.12	4236±116	324.8±6.5
H_β	2.88±0.13	5166±129	100.4±4.9
H_γ	1.13±0.05	5660±760	39.4±1.8
[O III]	0.59±0.04	898±22	19.4±1.9
[O II]	0.53±0.43	1042±88	14.2±1.4

Notes: Line flux in 10 $^{-15}$ ergs cm^{-2} s^{-1}, FWHM in km s^{-1} and rest-frame Equivalent Width (EW) in Å for the broad components of the Balmer lines, [OIII] and [OII].

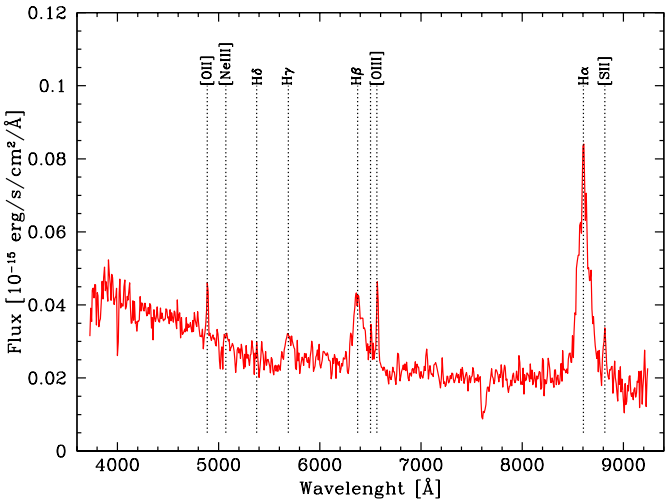

FIG. 4.— ESO NTT/EFOSC2 optical spectrum in the observer's frame. The main emission line wavelengths are indicated.

of the enigmatic class of naked AGNs that allegedly lack a BLR based on their unusual combination of spectral and temporal properties in the optical band (Hawkins 2004). The high-quality spectroscopic data presented in the previous section revealed the presence of strong broad lines in the optical spectrum of Q2122–444, ruling out its naked nature. Nevertheless, it is interesting to investigate the energetics of Q2122–444.

5.1. *Jet Contribution*

Before discussing the energetics of Q2122–444, it is important to establish whether a relativistic jet is present in this system and if its energetic contribution is important beyond the radio band. The original reason to look for a jet in Q2122–444 was that it represents the simplest solution to explain the unusual combination of spectral and temporal properties shown by Q2122–444 in the optical band. In this scenario, the jet not only

may produce the observed large-amplitude variability of the continuum but it can also contribute to the non-detection of broad optical lines through dilution. Additionally, the BLR emission could be partially obscured by a local absorber. However, the NTT/EFOSC2 optical spectroscopy has revealed that a BLR is indeed present in Q2122–444 and the X-ray spectral analysis has confirmed the lack of relevant intrinsic absorption. Nevertheless it is instructive to investigate the radio properties of this source to test the contribution of a putative jet.

The lack of radio detection in the ATCA observations leads to a 3 σ upper limit of 0.78 mJy for the radio flux of Q2122–444. This value combined with the flux measurements in the optical and X-ray bands yields low upper limits for the different radio-loudness parameters defined in the literature. For example, using the standard definition of radio loudness (e.g. Kellermann et al. 1994), we get $R \equiv L_\nu(5\ \mathrm{GHz})/L_\nu(\mathrm{B}) < 5.5$, which is well below the threshold $R = 10$ that is traditionally used to divide radio-quiet from radio-loud AGNs. Note however that $R = 10$ does not represent a reliable boundary between radio loud (RL) and radio quiet (RQ) AGNs (Ho & Peng 2001). A more reliable conclusion can be derived by using $R_\mathrm{x} \equiv \nu L_\nu(5\ \mathrm{GHz})/L_{2-10\ \mathrm{keV}}$, which was introduced by Terashima & Wilson (2003) to avoid extinction problems, and exploiting the results of Panessa et al. (2007), who carried out a detailed investigation of the radio loudness in two large samples of radio-quiet Seyfert galaxies and Low-Luminosity Radio Galaxies (LLRGs) and derived a RL/RQ threshold of $\log R_\mathrm{x} = -2.755 \pm 0.015$. The upper limit obtained for Q2122–444, $R_\mathrm{x} < 10^{-4}$, indicates that this source is fully consistent with radio-quiet Seyfert galaxies and inconsistent with radio-loud objects (see Figure 4 of Panessa et al. 2007). Since we have inferred that either a jet is absent in Q2122–444 or its contribution is completely negligible, for the remainder of the paper we can safely assume that the broadband emission is associated with the accretion flow only.

5.2. *Black Hole Mass*

The first necessary step to investigate the central engine in AGNs is to constrain the mass of the supermassive black hole. As with many AGNs for which there are no direct measurements from reverberation mapping, a BH mass of $\sim 2.2 \times 10^8\ M_\odot$ (Gliozzi et al. 2007) was determined using the virial theorem and FWHM([O III]), which however was proven to be not a very robust indicator of the stellar velocity dispersion (Netzer & Trakhtenbrot 2007). The broad Balmer lines detected in the EFOSC2 spectrum in combination with the simultaneously measured flux at 5100 Å, $f_{5100\mathring{A}} = (0.206 \pm 0.021) \times 10^{-16}$ erg cm^{-2} s^{-1} Å^{-1}, allows a more reliable estimate of M_BH. Plugging the value of FWHM(H_α) in the virial formula and using the relation between the broad line region radius and the 5100 Å luminosity from Bentz et al. (2009) to determine R_BLR, we derive $M_\mathrm{BH} = (7.1 \pm 1.4) \times 10^7\ M_\odot$, where a 20% error was conservatively adopted to account for the uncertainties associated with this method. Slightly larger values are obtained when using FWHM(H_β) and FWHM(H_γ) instead of FWHM(H_α): $M_\mathrm{BH} \simeq (9 - 10) \times 10^7\ M_\odot$.

An alternative way to constrain the M_BH of Q2122–444 is based on the analogy between AGNs and Galactic black holes (GBHs). There is now mounting evidence that AGNs may be considered as large-scale analogs of GBHs (e.g. Merloni et al. 2003; Falcke et al. 2004; Körding et al. 2006; McHardy et al. 2006). Despite the large difference in scales, both GBHs and AGNs are believed to harbor the same central engine: a black hole and an accretion disk/corona that sometimes produces a relativistic jet. It is also generally accepted that the bulk of the X-ray emission in any black hole system, irrespective of their mass, is produced by the Comptonization process, although some controversy still exists about the origin of X-rays during the low-hard state in GBHs (Zdziarski et al. 2003; Markoff et al. 2005). Recently, Shaposhnikov & Titarchuk (2009) discovered that GBHs during their spectral transition between low-hard to high-soft state present a universal scalable relationship between the photon index Γ and the normalization of the BMC model N_BMC, and that the $\Gamma - N_\mathrm{BMC}$ relationship can be used to estimate the mass of any GBHs.

The physical basis of these scaling techniques is thoroughly explained by Shaposhnikov & Titarchuk (2009) and essentially relies on the fact that the BMC normalization is a function of luminosity and distance ($N_\mathrm{BMC} \propto L/d^2$) and that the luminosity of a black hole system can be expressed as $L \propto \eta M_\mathrm{BH} \dot{m}$, where η is the radiative efficiency and $\dot{m}$ the accretion rate in Eddington units. The self-similarity of the N_BMC - Γ correlation shown by GBHs implies that, in the same spectral state, different sources have similar values of η and $\dot{m}$, and the photon index is a reliable indicator for the source's spectral state.

Since the Comptonization process producing the X-ray emission appears to be ubiquitous in black holes systems, and since there is evidence that the photon index is positively correlated with the accretion rate also in AGNs (e.g Shemmer et al. 2006; Papadakis et al. 2009), in principle, the same method may be applied to estimate the mass of supermassive black holes.

We have recently used this method to constrain M_BH in the particular case of the Narrow-line Seyfert 1 galaxy PKS 0558-504 (see Gliozzi et al. 2010 for details) and we are in the process of testing the extension of this method to SMBHs in general by applying it to a sizable sample of AGNs with masses determined via reverberation mapping (Gliozzi et al. in preparation). The basics steps of this scaling method can be summarized as follows:
1) Construct a $\Gamma - N_\mathrm{BMC}$ plot for a GBH of known mass and distance, which will be used as reference (hereafter denoted by the subscript r).
2) Compute the normalization ratio between the target of interest (that is denoted by the subscript t) and the reference object $N_\mathrm{BMC,t}/N_\mathrm{BMC,r}$ at the value of Γ measured for the target.
3) Derive the black hole mass using the following equation:

$$M_\mathrm{BH,t} = M_\mathrm{BH,r} \times (N_\mathrm{BMC,t}/N_\mathrm{BMC,r}) \times (d_t/d_r)^2 \times f_G \quad (1)$$

where $M_\mathrm{BH,r}$ is the black hole mass of the GBH reference object $N_\mathrm{BMC,t}$ and $N_\mathrm{BMC,r}$ are the respective BMC normalizations for the target (Q2122–444) and the reference source, d_t and d_r are the corresponding distances, and $f_G = \cos\theta_r / \cos\theta_t$ is the geometrical factor that depends on the respective inclination angles.

Using as a reference source GRO J1655-40, a well known microquasar whose parameters are tightly con-

strained – $M_{\rm BH}/M_{\odot} = 6.3\pm0.3, i = 70^o\pm1^o, d = 3.2\pm0.2$ kpc (Greene et al. 2001; Hjellming & Rupen 1995, but see Foellmi 2009 for a different estimate of the distance) – and assuming $f_G = 0.5$ which is appropriate considering that Q2122–444 has very likely a lower inclination angle compared to GRO J1655-40, we derive $M_{\rm BH} = (0.7-2.3)\times10^7\ M_{\odot}$ ($M_{\rm BH} = (2.8-6)\times10^7\ M_{\odot}$ when assuming $d_r = 2$ kpc). The range of masses reflects the 90% uncertainties on the spectral parameters Γ and $N_{\rm BMC}$. If GX 339-4, another prototypical GBH with $M_{\rm BH}/M_{\odot} = 12.3\pm1.4$, $d = 5.8\pm0.8$ kpc (Shaposhnikov & Titarchuk 2009), $i = 45^o-70^o$ (Kolehmainen & Done 2010), is used as a reference source, assuming again $f_G = 0.5$ we obtain $M_{\rm BH} = (2-8)\times10^7\ M_{\odot}$.

The values of $M_{\rm BH}$ obtained with this new method, which is independent of optical measurements and of any assumption on the BLR, appear to be in broad agreement with the values derived from the virial theorem. Although this consistency is encouraging, the robustness of the GBH scaling method needs to be quantitatively assessed using a large sample of AGNs. Therefore, for the remainder of the paper we will utilize the value determined from the H_{α} line and the virial theorem, $M_{\rm BH} \simeq 7\times10^7\ M_{\odot}$ This corresponds to an Eddington luminosity of $L_{\rm Edd} \simeq 9\times10^{45}$ erg s^{-1}.

5.3. *Energetics of Q2122–444*

In order to shed some light on the energetics Q2122–444, we will make use of some of the correlations determined by Lusso et al. (2010) from a detailed optical and X-ray study of a sample of 545 X-ray selected type 1 AGNs from the XMM-COSMOS survey. First, by using their Equation 6, which provides the relationship between $L_{2\ \rm keV}$ and $L_{2500\mathring{\rm A}}$, and Equation 9, which describes the correlation between $\alpha_{\rm OX}$ and $L_{2\ \rm keV}$, we can quantitatively verify whether the UV-to-X-ray properties of Q2122–444 are consistent with the those observed in "standard" type 1 AGNs. By plugging the value of $L_{2500\mathring{\rm A}}$ measured by the OM into Equation 6 of Lusso et al. (2010), we derive $\log L_{2\ \rm keV} = 25.05\pm1.16$ (where the quoted error reflects the uncertainty of the correlation parameters). This is in full agreement with $\log L_{2\ \rm keV} = 24.97$, the value determined from the EPIC pn measurement. Similarly, by plugging the measured value of $L_{2\ \rm keV}$ into Equation 9 of Lusso et al. (2010), we derive $\alpha_{\rm OX} = 1.34\pm0.65$, which again is in agreement with the value inferred from the simultaneous measurements of the EPIC cameras and the OM aboard *XMM-Newton*, $\alpha_{\rm OX} = 1.31$.

Since in the UV-X-ray regime Q2122–444 behaves as a typical type 1 AGN, we can exploit the relationship between the X-ray bolometric correction $\kappa_{\rm bol} \equiv L_{2-10\ \rm keV}/L_{\rm bol}$ and $\alpha_{\rm OX}$ presented by Lusso et al. (2010) to derive the bolometric luminosity of Q2122–444. By plugging $\alpha_{\rm OX} = 1.31$ into Equation 11 of Lusso et al. (2010), we infer $\kappa_{\rm bol} = 17.3$, which combined with the measured value of $L_{2-10\ \rm keV}$ leads to $L_{\rm bol} \simeq 2\times10^{44}$ erg s^{-1}. The bolometric luminosity in turn can be used to constrain the accretion rate of Q2122–444 in terms of Eddington units. Specifically, dividing $L_{\rm bol}$ by the Eddington luminosity we determine $\lambda_{\rm Edd} \equiv L_{\rm bol}/L_{\rm Edd} \simeq 2\times10^{-2}$, which appears to be typical for "normal" type 1 AGNs but fairly large when compared with the values inferred for the few confirmed true type 2 AGNs (e.g. Bianchi et al. 2008; Panessa et al. 2009; Shi et al. 2010).

Finally, we can exploit the relationship between $\lambda_{\rm Edd}$ and $\kappa_{\rm bol}$ from Lusso et al. (2010) to test our estimate of the BH mass. More specifically, if we invert Equation (14) of Lusso et al. (2010) and thus express $\lambda_{\rm Edd}$ as a function of the bolometric correction $\kappa_{\rm bol}$, we derive $\lambda_{\rm Edd} = (6\pm2)\times10^{-2}$. This is consistent with the value inferred above that was obtained using $M_{\rm BH} = 7\times10^7\ M_{\odot}$ and hence provides an indirect confirmation of the validity of the mass estimate.

6. CONCLUSION

We have used data from a long *XMM-Newton* exposure complemented with an *ATCA* radio observation and with high-quality optical spectroscopic data from the ESOFC2/NTT to investigate in details the nature of the putative naked AGN Q2122–444. The main results can be summarized as follows.

- A thorough spectroscopic analysis of the NTT/EFOSC2 data reveals the presence of strong broad H_{α}, H_{β}, and H_{γ} lines that are in stark contrast with the prior classification of Hawkins (2004) based on low S/N spectra. We can therefore rule out at high confidence level that, at the time of the NTT/EFOSC2 observation in June 2009, Q2122–444 was lacking a regular BLR.

- The lack of detection of any radio emission and the consequent low value of the upper limit of the radio loudness implies that a relativistic jet (postulated to explain the long-term optical variability observed for over two decades in Q2122–444) is unlikely to be present and certainly does not play a relevant role in the energetics of this AGN.

- A temporal X-ray analysis indicates that Q2122–444 remains constant in the 0.3–10 keV energy band on timescales of a few ks. On the other hand, a comparison with a *Chandra* observation carried out nearly two years before the *XMM-Newton* pointing reveals the presence of significant flux variability accompanied by moderate spectral variability. Q2122–444 appears to follow the typical spectral variability trend observed in Seyfert 1 galaxies, with a steeper X-ray spectrum when the source is brighter.

- A spectral analysis of the combined EPIC spectra confirms the *Chandra* results that suggested that 0.4-10 keV spectrum of Q2122–444 was featureless and adequately fitted by a simple power-law. The higher quality of the *XMM-Newton* spectral data makes it possible to tightly constrain the spectral parameters and indicates that the intrinsic absorption is negligible.

- From the measurement of FWHM(H_{α}) and the virial theorem we estimate for Q2122–444 $M_{\rm BH} = (7.1\pm1.4)\times10^7\ M_{\odot}$. Similar values are obtained by applying a new scaling technique recently developed for GBHs and based on the results of the X-ray spectral fit with a Comptonization model.

- We use the optical-to-X-ray properties of Q2122–444 derived from simultaneous observations of the EPIC cameras and the OM aboard *XMM-Newton* to investigate the energetics of this source. To this end and to put Q2122–444 in context, we exploit the correlations derived by Lusso et al. (2010) for a large sample of AGNs from the XMM-COSMOS survey. With a bolometric luminosity of $L_{\rm bol} \simeq 2\times10^{44}$ erg s^{-1} and an accreting rate in Eddington units of $\lambda_{\rm Edd} \simeq 2\times10^{-2}$ Q2122–444 appears to be fully consistent with standard type 1 AGNs and at odds with the few confirmed true type 2 AGNs.

In summary, our analysis indicates that Q2122–444 is not a true type 2 AGN, since the presence of a BLR is clearly demonstrated. The relatively high accretion rate and high X-ray luminosity of Q2122–444 compared to the confirmed true type 2 AGNs argues against an intrinsic variability scenario where the optical classification may change on timescales of years. In this specific case, the original classification as a naked AGN appears to be more likely ascribed to a low S/N spectrum and/or to an obscuring event during the first optical observation. Of the six "naked AGN" originally selected by Hawkins (2004), three have been observed with deep X-ray observations coupled with high S/N optical spectroscopy and only one, Q2131-427, confirmed the genuine lack of a BLR. Our findings highlight the need of high-quality X-ray and optical spectroscopic data to robustly classify true type 2 AGNs and seem to confirm that these type of objects are indeed rare, although a systematic analysis of a large sample of AGNs is necessary in order to derive more general conclusions.

We thank the anonymous referee for the very constructive suggestions that have improved the clarity of the paper. MG acknowledges support by the XMM-Newton Guest Investigator Program under NASA grant NNX08AB67G and by the NASA ADP grant NNXlOAD51G. We thank Ranjani Sarma for helping with the X-ray spectral analysis.

REFERENCES

Antonucci, R. 1993, ARA&A, 31, 473
Arnaud, K. 1996, in ASP Conf. Ser. 101, Astronomical Data Analysis Software and Systems V, ed. G. Jacoby & J. Barnes (San Francisco: ASP), 17
Bentz, M.C. et al. 2009, ApJ, 697, 160
Bian, W. & Gu, Q. 2007, ApJ, 657, 159
Bianchi, S., et al. 2008, MNRAS, 385, 195
Cardelli, J.A., Clayton, G.C., & Mathis, J.S. 1989, ApJ, 345, 245
Cox, A.N. & Allen, C.W. 2000, Allen's Astrophysical Quantities, IV edition (New York: AIP)
Diamond-Stanic, A.M., et al. 2009, ApJ, 669, 782
Elitzur, M. & Ho, L.C. 2009, ApJ, 701, L91
Falcke, H., Körding, E., & Markoff, S. 2004, A&A, 414, 895
Foellmi, C. 2009, NweA, 14, 674
Gliozzi, M., Sambruna, R.M., & Foschini, L. 2007, ApJ, 662, 878
Gliozzi, M., et al. 2010, ApJ, 717, 1243
Greene, J., Bailyn, C.D., & Orosz, J.A. 2001, ApJ, 554, 1290
Gu, Q. & Huang, J. 2002, ApJ, 579, 205
Hawkins, M.R.S. 2004 A&A, 424, 519
Hjellming, R.M. & Rupen, M.P. 1995, Nature, 375, 464
Ho, L.C. & Peng, C.Y. 2001,ApJ, 555, 650
Hopkins, P.F.,Strauss, M.A., Hall, P.B., et al. 2004, AJ, 128, 1112
Kellermann, K.I., Sramek, R.A., Schmidt, M., Green, R.F., & Shaffer, D.B. 1994, AJ, 98, 1195
Körding, E.G., Jester, S., & Fender, R.P. 2006, MNRAS, 372, 1366
Kolehmainen, M. & Done, C. 2010, MNRAS, 406, 2206
Lawrence, A.& Elvis, M. 1982, ApJ, 256, 410
La Franca, F., et al. 2005, ApJ, 635, 864
Lissandrini, C., Cristiani, S., & La Franca, F. Astronomical Society of the Pacific, Publications (ISSN 0004-6280), vol. 106, no. 705, p. 1157-1164
Lusso, E., et al. 2010, A&A, 512A, 34
Markoff, S., Nowak, & M., Wilms, J. 2005, ApJ, 635, 1203
Mason, K.O., et al. 2001, A&A, 365, L36
McHardy, I.M., Körding, E.G., Knigge, C., Uttley, P., & Fender, R.P. 2006, Nature, 444, 730
Merloni, A., Heinz S., & di Matteo, T. 2003, MNRAS, 345, 1057
Nenkova, M., Ivezi¸, & Elizur, M. 2002, ApJ, 570, L9
Netzer, H. & Trakhtenbrot, B. 2007, ApJ, 654, 754
Nicastro, F. 2000, ApJ, 530, L65
Osterbrock, D.E. 1981, ApJ, 249, 4620
Panessa F., Bassani L., 2002, A&A, 394, 435
Panessa, F., et al. 2007, A&A, 467, 519
Panessa, F., et al. 2009, MNRAS, 398, 1951
Papadakis, I.E., et al. 2009, A&A, 494, 905
Pappa A., Georgantopoulos I., Stewart G. C., Zezas A. L., 2001, MNRAS, 326, 995
Plotkin, R.M., et al. 2010, ApJ, 721, 562
Prévot, M.L., Lequex, J., Maurice, E., Prévot, L., & Rocca-Volmerange B. 1984, A&A, 132, 389
Risaliti, G., et al. 2009, MNRAS, 393, L1
Shaposhnikov, N. & Titarchuk, L. 2009, ApJ,699, 453
Shemmer, O., Brandt, W.N., Netzer, H., Maiolino, R., & Kaspi, S. 2006, ApJ, 646
Shi, Y. et al.2010, ApJ, 714, 115
Sobolewska, M.A. & Papadakis, I.E. 2009, MNRAS, 339, 1597
Steffen, A.T., Barger, A.J., Cowie, L.L., Mushotzky, R.F., & Yang, Y. 2003, ApJ, 596, L23
Tananbaum, H., Avni, Y., Branduardi, G., et al. 1979, ApJ, 234, 9L
Terashima, Y. & Wilson, A.S. 2003, ApJ, 583, 145
Titarchuk, L.G., Mastichiadis, A. & Kylafis, N.D. 1997, ApJ, 487, 834
Tran, H.D. 2001, ApJ, 554, L19
Trump, J.R., et al. 2009, ApJ, 706, 797
Turner, T.J., George, I.M., Nandra, K., & Mushotzky, R.F. 1997, ApJS, 113, 23
Urry, C.M. & Padovani, P. 1995, PASP, 107, 803
Watson, F., Offer, A.R., Lewis, I.J., Bailey, J.A., & Glazebrook, K. Fiber Optics in Astronomy III. ASP Conference Series, Vol. 152, 1998, ed. S. Arribas, E. Mediavilla, and F. Watson (1998). Proceedings of a meeting held in Puerto de la Cruz, Canary Islands, Spain, 2-4 December 1997. ISBN 1-886733-72-4., p.50
Zdziarski, A.A., Lubiǹski, P., Gilfanov, M & Revnivtsev, M. 2003, MNRAS, 342, 355
Zombeck, M.V. 1990, Handbook of Space Astronomy and Astrophysics (Cambridge: Cambridge Univ. Press)